Environmental Science & Technology

Article

Cite This: Environ. Sci. Technol. 2020, 54, 184−194

pubs.acs.org/est

A Rapid Assay to Assess Nitrification Inhibition Using a Panel of Bacterial Strains and Partial Least Squares Modeling

Patrick Morkus, Mehdi Zolfaghari, Salman Alizadeh Kordkandi, Jake Nease, Carlos D. M. Filipe, and David R. Latulippe*

Department of Chemical Engineering, McMaster University, 1280 Main Street West, Hamilton, Ontario L8S 4L7, Canada

Supporting Information

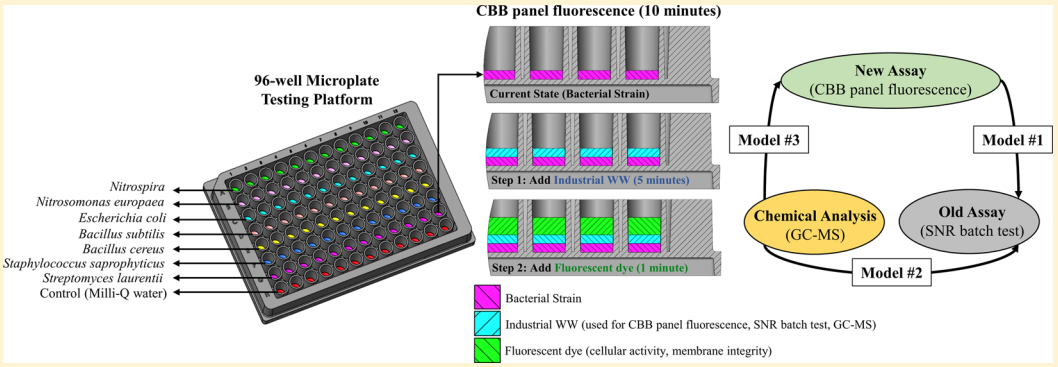

ABSTRACT: As a proof of concept, a rapid assay consisting of a cell-based biosensor (CBB) panel of pure bacterial strains, a fluorescent dye, and partial least squares (PLS) modeling was developed to assess the nitrification inhibition potential of industrial wastewater (WW) samples. The current standard method used to assess the nitrification inhibition potential is the specific nitrification rate (SNR) batch test, which requires approximately 4 h to complete under the watch of an experienced operator. In this study, we exposed the CBB panel of seven bacterial strains (nitrifying and non-nitrifying) to 28 different industrial WW samples and then probed both the membrane integrity and cellular activity using a commercially available "live/dead" fluorescent dye. The CBB panel response acts as a surrogate measurement for the performance of nitrification. Of the seven strains, four (*Nitrospira*, *Escherichia coli*, *Bacillus subtilis*, *Bacillus cereus*) were identified via the modeling technique to be the most significant contributors for predicting the nitrification inhibition potential. The key outcome from this work is that the CBB panel fluorescence data (collected in approximately 10 min) can accurately predict the outcome of an SNR batch test (that takes 4 h) when performed with the same WW samples and has a strong potential to approximate the chemical composition of these WW samples using PLS modeling. Overall, this is a powerful technique that can be used for point-of-use detection of nitrification inhibition.

1. INTRODUCTION

Nitrification, the biologically mediated process of converting ammonia to nitrate, is widely used in municipal wastewater treatment plants (WWTPs) to meet strict ammonia effluent limits. Nitrifying microorganisms (i.e., nitrifiers), including *Nitrosomonas europaea* and *Nitrospira*, have been found in the activated sludge of WWTPs.[1−3] The rate of nitrification can be negatively affected by the presence of various chemical compounds in the influent to the municipal WWTP.[4] A variety of manufacturing plants from the food, automotive, pharmaceutical, metal working, and other industries use biocides (which include insecticides, fungicides, herbicides, acaricides) to enhance process performance by inhibiting microbial growth, inhibiting equipment corrosion, and other associated effects.[5−8] The wastewaters (WWs) generated by these industries are usually pretreated in industrial WWTPs prior to being directed to municipal WWTPs.[9] It is critical that an assessment of the potential effect of those incoming sources on the performance of the municipal WWTP is made; ideally, this assessment should be (1) fairly simple to conduct, (2) fairly rapid in response, and (3) able to identify the source of the inhibitory chemical compounds. The current "gold-standard" method to assess nitrification inhibition is the specific nitrification rate (SNR) batch test.[10] This is a laborious method requiring frequent measurements of nitrate and nitrite concentrations, with and without the presence of potential nitrification inhibitors, over a few hours of operation. A rapid test to assess the toxicity of such WW sources would be beneficial to the operation of municipal WWTPs and could also be used for monitoring "point-of-use" of biocides at industrial/commercial facilities. Also, the SNR batch test gives no information about the source of the nitrification

Received: July 24, 2019
Revised: November 11, 2019
Accepted: December 2, 2019
Published: December 2, 2019

DOI: 10.1021/acs.est.9b04453
Environ. Sci. Technol. 2020, 54, 184−194

inhibition. Thus, additional testing using sophisticated equipment, such as liquid chromatography−mass spectrometry (LC-MS) and/or gas chromatography−mass spectrometry (GC-MS), is used.[11] The complexity, time requirement, and large cost associated with this additional testing have created a space for innovating simpler methods/assays capable of assessing toxicity specifically with respect to nitrification inhibition.

Due to their relatively low-cost and rapid response kinetics, cell-based biosensors (CBBs) have gained significant attention for various applications in food, medical, environmental, and other industries.[12,13] In the environmental field specifically, the potential toxicity of various chemical compounds in water and soil samples has been determined using CBBs based on different microorganisms. For example, multi-bacterial toxicity assays such as MARA[14] and LumiMARA,[15] which use absorbance and bioluminescence respectively, have been used to assess the toxicity of environmental samples. However, these assays have not been used to assess nitrification. As another example, commercially available tests using bioluminescent *Vibrio fischeri* have been used to measure the toxicity of metals in environmental samples[16] and the concentration of biocides in paper mill process waters.[17] *Vibrio fischeri* has also been tested for its ability to predict the kinetics of nitrification with some success;[18] however, the long test time (approximately 1.5 h) and the inability to assess the source of inhibition are the major limitations of this technique. This technique also does not consider the response of the nitrifying organisms which are responsible for nitrification. Nitrification inhibition assays based on pure cultures of *Nitrosomonas* and *Nitrobacter* were developed and tested on influent samples to municipal WWTPs[19] and industrial WW samples.[20,21] However, these pure culture assays still required the same amount of time (4 h) as a conventional activated sludge assay.

In order to solve the problem of developing a rapid assay to assess nitrification inhibition, we were inspired by the development of "soft sensor" technologies that have been used in various manufacturing industries to predict difficult-to-measure response variables using easy-to-measure process parameters.[22,23] For example, in the biotechnology industry, multiwavelength fluorescence spectra trajectories have been used to monitor cell densities, recombinant protein concentrations, and other time-consuming and/or difficult-to-measure components in mammalian cell cultures.[24] In another case, oxidation reduction potential and pH measurements were used to monitor for nitrogen and phosphorus removal in the biological treatment of municipal WW.[25]

In this study, we selected a diverse panel of seven bacterial strains (e.g., Gram-negative/Gram-positive, oval-shaped/rod-shaped, nitrifying): *Nitrospira*, *Nitrosomonas europaea*, *Escherichia coli*, *Bacillus subtilis*, *Bacillus cereus*, *Staphylococcus saprophyticus*, and *Streptomyces laurentii*. We used a fluorescent cell dye (SYTO 9, propidium iodide) to monitor for changes in membrane integrity and cellular activity after exposure to a "library" of industrial WW samples. This fluorescence cell dye is known for its ability to probe for intact and disrupted cytoplasmic membranes.[26−28] Also, because the dye binds to DNA and RNA,[29] it is hypothesized that this method would also probe for cellular activity (e.g., expression of genes upon the cell's exposure to stress).[30,31] Therefore, the combination of these two effects is anticipated to provide information about the interaction between each strain and the chemical compounds present in a WW sample. Furthermore, because each strain (both nitrifying and non-nitrifying) behaves differently, combining the information from each strain allows for a greater understanding of the repercussions of the WW sample on bacteria that can be used as a surrogate measurement—in combination with a model—for the performance of various cellular functions (e.g., nitrification). The key advantage to this approach is that the CBB panel fluorescence data for all of the strains can be collected in approximately 10 min. In parallel to this work, we obtained SNR batch test and GC-MS data for the same "library" of WW samples. By combining all of these data/results (CBB panel fluorescence, SNR batch test, GC-MS) and partial least squares (PLS) modeling, we are able to predict the SNR outcomes with a strong potential to approximate the chemical composition of the WW samples.

2. MATERIALS AND METHODS

2.1. Preparation of Bacterial Strains. Seven bacterial strains were used in this study:

- *Nitrospira*, a Gram-negative and common aerobic chemolithoautotroph bacterium, was purchased from DSMZ (Braunschweig, Germany). *Nitrospira* has been commonly found in activated sludge (approximately 9% of total bacterial count) of WWTPs and is responsible for oxidizing nitrite to nitrate.[32] *Nitrospira* were grown at 28 °C over 4 weeks; it should be noted that the culturing conditions could be optimized to reduce the amount of time needed.[33] For the first 2 days, a Thermo MaxQ 8000 shaker incubator was used to shake the bacteria-media solution (see below) in a 100 mL Erlenmeyer flask set at 225 rpm to improve oxygen uptake; no shaking was done for the remainder of the 4 weeks. The media solution was made (as per DSMZ recommendations) by dissolving EDTA (1.4 mg/L), KH_2PO_4 (1.4 mg/L), $MgSO_4{\cdot}7H_2O$ (100 mg/L), $CaCl_2{\cdot}2H_2O$ (10 mg/L), $FeSO_4$ (5 mg/L), $NaNO_2$ (212 mg/L), K_2CO_3 (258 mg/L), $CuSO_4{\cdot}5H_2O$ (0.1 mg/L), $MnCl_2$ (1 mg/L), $ZnSO_4{\cdot}7H_2O$ (0.5 mg/L), and $Na_2MoO_4{\cdot}H_2O$ (0.5 mg/L) in Milli-Q water. All the chemicals used were of analytical grade.
- *Nitrosomonas europaea*, a Gram-negative obligate chemolithoautotroph bacterium, was also purchased from DSMZ. It has been found in activated sludge of WWTPs and operates under aerobic conditions oxidizing ammonia to nitrite.[3] *N. europaea* uses only ammonia as energy and only carbon dioxide as cellular carbon to function.[34] *N. europaea* were grown at 28 °C over 4 weeks (no shaking) in a 100 mL Erlenmeyer flask containing a media solution that was made (as per DSMZ recommendations) by dissolving Cresol red (1000 mg/L), KH_2PO_4 (54 mg/L), $MgSO_4{\cdot}7H_2O$ (49 mg/L), $CaCl_2{\cdot}2H_2O$ (147 mg/L), $FeSO_4$ (1 mg/L), NH_4Cl (535 mg/L), $NaHCO_3$ (1306.9 mg/L), NaCl (584 mg/L), and KCl (74 mg/L) in Milli-Q water. This solution was replenished once per week. All the chemicals used were of analytical grade.
- *Escherichia coli DH5α*, an abundant Gram-negative facultative aerobic bacterium, was provided by the Biointerfaces Institute at McMaster University. It has been shown that the amount of *E. coli* can reach levels of approximately 10^3 to 10^5 cells per gram of activated sludge.[35] *E. coli* were grown for 20 h in Lysogeny broth (LB) media (Sigma-Aldrich) in 14 mL polystyrene round-bottom Falcon tubes at 37 °C in a Thermo MaxQ 8000 shaker incubator set at 225 rpm.

DOI: 10.1021/acs.est.9b04453
Environ. Sci. Technol. 2020, 54, 184−194

- *Bacillus subtilis*, a Gram-positive aerobic bacterium that can grow in diverse environments, was provided by the Biointerfaces Institute at McMaster University. *B. subtilis* was included due to its role in bioflocculant production which is known to occur in activated sludge during the aeration process.[36] *B. subtilis* were grown for 20 h in LB media in 14 mL polystyrene round-bottom Falcon tubes at 26 °C in a Thermo MaxQ 8000 shaker incubator set at 225 rpm.
- *Bacillus cereus*, a Gram-positive aerobic and facultative anaerobic bacterium, was provided by the Agricultural Research Service Culture Collection (Peoria, IL). *B. cereus* is commonly found in a variety of environments and has been confirmed to exist in soils, water, food and activated sludge of WWTPs.[37] *B. cereus* were grown under the exact same conditions as given above for *B. subtilis*.
- *Staphylococcus saprophyticus*, a Gram-positive bacterium, was provided by the Biointerfaces Institute at McMaster University. *S. saprophyticus* belongs to the class *Staphylococci* which are commonly found in activated sludge of WWTPs.[38,39] In cases where biological aerobic treatment of saline WW is required, *Staphylococci* can act as a supplement in activated sludge to improve chemical oxygen demand (COD) removal rates.[40] *S. saprophyticus* were grown for 20 h in Tryptic Soy Broth media (Sigma-Aldrich) in 14 mL polystyrene round-bottom Falcon tubes at 37 °C in a Thermo MaxQ 8000 shaker incubator set at 225 rpm.
- *Streptomyces laurentii*, a Gram-positive bacterium, was provided by the NRRL. *S. laurentii* can be typically found in soil and belongs to the class *Streptomyces* which are Gram-positive aerobic mycelial bacteria.[41] *Streptomyces* are also known to contribute to the removal of heavy metals, biological oxygen demand (BOD), and total suspended solids (TSS) from WW.[42] *S. saprophyticus* were grown for 20 h in Tryptic Soy Broth media (Sigma-Aldrich) in 14 mL polystyrene round-bottom Falcon tubes at 26 °C in a Thermo MaxQ 8000 shaker incubator set at 225 rpm.

The resulting bacteria-media solutions were transferred into 50 mL polystyrene Falcon tubes and then centrifuged at 8 °C and 4000 rpm for 16 min. The supernatant was replaced with an equal volume of phosphate buffered saline (PBS) solution (BioShop) to make bacterial cell stocks. In order to confirm that the correct bacteria were received and successfully grown at the reported conditions, 10 μL aliquots of each cell stock were sent to the Mobix Lab at McMaster University for Sanger sequencing of the 16S rRNA gene. Each aliquot was prepared for sequencing according to the following three-step sequence: boiling at 95 °C for 15 min; PCR amplification using 8f (5′-AGAGTTTGATCCTGGCTCAG-3′) and 926r (5′-CCGTCAATTCCTTTRAGTTT-3′) primers; column purification using the PureLink PCR Purification kit (Invitrogen). The strains were identified using BLAST search software, and all achieved a 99% identity to that which was expected.

2.2. Fluorescence Assay: CBB Panel Exposure to Wastewater. Twenty-eight WW samples were obtained from an industrial WWTP that receives WW derived from over 100 different clients from a variety of chemical, food, automotive, and other industries and discharges the treated WW at varying volumes (approximately 200000−500000 L per day) to a local municipal WWTP. The samples used in this study were treated physicochemically (e.g., flocculation-coagulation, hydrogen peroxide with aeration, sand filtration, adsorption via clay or activated carbon) at the industrial WWTP. The samples were collected over a period of approximately two months to help ensure diversity in the samples. Before testing, each WW sample was first centrifuged at 4000 rpm for 16 min to remove any suspended solid material.

Duplicate 50 μL aliquots of the supernatant from each WW sample were transferred into individual wells of a 96-well flat bottom black microplate (Eppendorf); duplicate 50 μL aliquots of Milli-Q water were also added to separate wells of the microplate as negative controls. An 8-channel pipet was used to add 50 μL of each bacterial cell stock into each well being tested. After 5 min, 100 μL of the LIVE/DEAD *Bac*Light dye solution (prepared according to the manufacturer's instructions for the L7007 Bacterial Viability Kit) was added to each well using an 8-channel pipet; this step was completed in less than 1 min. The fluorescence signals of the contents within the 96-well microplate were determined using an Infinite M200 Pro multimode microplate reader (Tecan) at the following settings: shaking frequency of 2 min, shaking time of 30 s, default gain of 60, excitation wavelength of 485 nm, emission wavelength of 530 nm. The reported fluorescence signals for a given combination of bacteria and WW were obtained by subtracting the "background" corresponding to the fluorescence signal from those wells containing only the WW and dye solution (i.e., no bacteria).

The fluorescence signals for each bacterial strain exposed to Milli-Q water (control) were 2900 ± 50, 2300 ± 25, 6100 ± 50, 19000 ± 500, 8800 ± 400, 4700 ± 50, and 24000 ± 100 relative fluorescence units (RFU) for *Nitrospira*, *Nitrosomonas europaea*, *Escherichia coli*, *Bacillus subtilis*, *Bacillus cereus*, *Staphylococcus saprophyticus*, and *Streptomyces laurentii*, respectively (Figure S1). The differences in fluorescence readings were due to the differences in bacterial concentrations from strain to strain which was a result of implementing a convenient 20-h growth period for all strains (except for *Nitrospira* and *N. europaea* which was 4 weeks) regardless of their varying growth mediums and growth temperatures.[43] In our preliminary testing (results not shown), we found that it was difficult to differentiate fluorescence signals of the same bacterial strain when exposed to different WW samples if a low control fluorescence signal (<1000) was used.

2.3. SNR Batch Test Assay. The SNR batch test assay used in this study was adapted from Bye et al.[10] As shown in Figure S2, eight 100 mL Erlenmeyer flasks were used to simultaneously test eight samples (typically seven WW samples and one Milli-Q water control). The following components were added to each flask:

- An 85 mL aliquot of return activated sludge (RAS) from the Dundas Valley WWTP in Dundas, Ontario. The as-received RAS was concentrated via a simple batch centrifugation process to achieve a volatile suspended solids (VSS) value, as per Method 1684,[44] in the range of 4400−5400 mg/L, which is typical in WWTPs.[45,46]
- A 10 mL aliquot of a synthetic mineral medium solution made in Milli-Q water (as per Seyhi et al.[47]) with the following chemicals (all of analytical grade) at the given concentrations: KH_2PO_4 (355 mg/L), $MgSO_4{\cdot}7H_2O$ (203 mg/L), $CaCl_2{\cdot}2H_2O$ (366 mg/L), $FeCl_3$ (15 mg/L), NH_4Cl (1920 mg/L), $NaHCO_3$ (421 mg/L), $CuSO_4{\cdot}$

DOI: 10.1021/acs.est.9b04453
Environ. Sci. Technol. 2020, 54, 184−194

$5H_2O$ (0.4 mg/L), $MnSO_4{\cdot}4H_2O$ (0.4 mg/L), $ZnSO_4{\cdot}7H_2O$ (0.4 mg/L), and $Na_2MoO_4{\cdot}H_2O$ (0.25 mg/L).

- A 5 mL aliquot of CH_3COONa solution (2970 mg/L in Milli-Q water) was used as a source of COD.

To start the SNR batch test, a 0.6 mL aliquot of the WW sample (or Milli-Q water for the control) was added to the mixture of components in each flask and then the air supply was immediately turned on; as shown in Figure S2, a custom-made manifold was used to deliver the air from a single supply to all eight flasks. The amount of dissolved oxygen within each flask was continuously monitored using a YSI 5000 dissolved oxygen meter to be in the range of 8 to 9 mg/L. The solution pH was continuously monitored via a VWR Benchtop pH meter and adjusted via the addition of 0.1 N H_2SO_4 solution (Sigma-Aldrich) to be in the pH range of 7 to 8; the maximum amount of acid added to any flask was 4 mL. A 1 mL sample was taken from each flask at three different time points (20, 45, and 75 min) after the air supply was turned on. Each sample was first centrifuged at 2000 rpm for 5 min, and then the nitrite-N and nitrate-N concentrations of the resulting supernatant were determined using a Nitrite TNTplus Vial Test HR kit (HACH), a NitraVer X Nitrogen-Nitrate Reagent Set HR kit (HACH), and a DR-2800 spectrophotometer (HACH).

The SNR for each sample was determined from the slope of NO_x-N (total concentration (in mg/L) of nitrite-N and nitrate-N) versus time divided by the initial concentration (g/L) of VSS. According to Raboni et al.,[48] the measured SNR values were normalized to 20 °C via the following:

$$\mathrm{SNR}_{20^\circ\mathrm{C}} = \frac{\mathrm{SNR}_T}{1.07^{T-20}} \quad (1)$$

where T is the average temperature (in °C) that was measured using a standard glass thermometer throughout the 75 min test. The % SNR difference was then calculated using

$$\%\ \text{SNR difference} = \frac{\mathrm{SNR}_{20^\circ\mathrm{C}}(\text{sample}) - \mathrm{SNR}_{20^\circ\mathrm{C}}(\text{control})}{\text{Average}(\mathrm{SNR}_{20^\circ\mathrm{C}}(\text{sample}),\ \mathrm{SNR}_{20^\circ\mathrm{C}}(\text{control}))} \quad (2)$$

From this, a % SNR difference of less than zero implies nitrification was not inhibited while a % SNR difference of greater than zero implies nitrification was inhibited. The acceptable level of nitrification inhibition will vary depending on the discharge limits of different jurisdictions.[49]

2.4. Gas Chromatography Mass Spectrometry (GC-MS) Analysis. A 100 mL aliquot of each industrial WW sample was pH-adjusted to 2.0 ± 0.2 via the addition of 1 N HCl solution (LabChem); this mixture was then combined with 100 mL of dichloromethane (DCM) (Caledon) in a separatory funnel, manually shaken for 1 min, then allowed to rest for 5 min in order to partition into two separate phases. Approximately 100 mL of the bottom DCM rich phase was extracted from the separatory funnel and then dehydrated by pouring it through approximately 5 g of anhydrous sodium sulfate (Anachemia) on top of a 30 μm Whatman filter paper in a glass funnel. The dehydrated and filtered sample was then concentrated to 2 mL using a rotary vacuum evaporator operated at 37 °C. A 25 μL aliquot from the concentrated 2 mL sample was combined with 25 μL of *N*-methyl-*N*-trimethylsilyl-trifluoroacetamide (MSTFA) (Sigma-Aldrich) containing 1% trimethylchlorosilane (Fluka) and 5 μL of 9-anthracenemethanol (Sigma-Aldrich) in a 2 mL Clear Robo vial; 9-anthracenemethanol was included as an "internal standard" for the GC-MS analysis. This mixture was then placed in a 60 °C oven for 1 h. The GC-MS analysis was performed using a 6890N gas chromatograph (Agilent) equipped with a DB-17ht column (30 m × 0.25 mm ID × 0.15 μm film, J & W Scientific) with a retention gap (deactivated fused silica, 5 m × 0.53 mm ID) and a 5973 MSD single quadruple mass spectrometer (Agilent). A 1 μL aliquot of the sample was injected into the chromatograph using a 7683 autosampler (Agilent) in splitless mode. The injector temperature was 250 °C, and the carrier gas (helium) flow rate was 1.1 mL/min. The transfer line temperature was 280 °C, and the MS source temperature was 230 °C. The column temperature was initially set at 50 °C which was then increased to 300 °C via an 8 °C/min ramp and held at 300 °C for 15 min for a total run time of 46.25 min. A full scan mass spectra between a mass-to-charge ratio of 50 and 800 was acquired; the multichannel ion detector was turned off during the 0−2.5 and 2.8−3.9 min marks for toluene (solvent used as the stationary phase when the injection mode is splitless) and MSTFA, respectively.

2.5. Partial Least Squares (PLS) Modeling. The PLS modeling was conducted using Aspen ProMV software (AspenTech) which uses the nonlinear iterative partial least-squares (NIPALS) algorithm.[50] For a detailed review of the mathematics and standard notation of PLS modeling, the reader is referred to the earlier work by Höskuldsson.[51] Three separate PLS models were developed in this study:

1 CBB to SNR: this is the main model (i.e., "soft sensor") that was used to predict the % SNR difference based on the fluorescence signal of the CBB panel. The model input (*X*-space) contains the bacterial strains as variables (columns) and WW samples as observations (rows). The fluorescence signal for each bacterial strain and for each WW sample fills the *X*-space. The model output (*Y*-space) contains the % SNR difference as the only variable (column) and the same WW samples as observations (rows). Weight matrices, which define the orientation of the principal components, were labeled as 'W' for the CBB *X*-space and 'c' for the SNR *Y*-space; see Figure S3 for a schematic representation.

2 GC-MS to SNR: this model was used to determine which of the chemical compounds in the WW samples (Table S2) contributed to nitrification inhibition. The model input (*X*-space) contains the chemical compounds as variables (columns) and WW samples as observations (rows). Standardized GC-MS peak area values fill the *X*-space; the integral area for each peak (i.e., chemical compound) was divided by the integral area of the internal standard (see Table S2). The model output (*Y*-space) contains the % SNR difference as the only variable (column) and the same WW samples as observations (rows). Weight matrices which define the orientation of the principal components were labeled as 'W' for the GC-MS *X*-space and 'c' for the SNR *Y*-space; see Figure S4 for a schematic representation.

3 GC-MS to CBB: this model was used to determine which of the chemical compounds in the WW samples (Table S2) contributed to a change in the fluorescence signals for two (*Nitrospira*, *Escherichia coli*) of the seven bacterial strains. The model input (*X*-space) contains the chemical compounds as variables (columns) and WW samples as observations (rows). Standardized GC-MS peak area values fill the *X*-space; the integral area for each peak (i.e., chemical compound) was divided by the integral area of

DOI: 10.1021/acs.est.9b04453
Environ. Sci. Technol. 2020, 54, 184−194

the internal standard. The model output (*Y*-space) contains the two bacterial strains mentioned above as the variables (columns) and the same WW samples as observations (rows). Weight matrices which define the orientation of the principal components were labeled as 'W' for the GC-MS *X*-space and 'c' for the CBB subset *Y*-space; see Figure S5 for a schematic representation.

3. RESULTS AND DISCUSSION

3.1. CBB Panel Fluorescence and SNR Batch Tests. The results collected from the CBB panel and SNR batch test for one of the industrial WW samples (WW #4) are shown in Figure 1. The fluorescence signals from the CBB panel are shown in the panel on the left. A microplate reader was used to record the fluorescence signals over a 15 min reading period (as per the instructions provided by the manufacturer of the dye); however, it was found that only the initial fluorescence signal, which was retrieved 1 min after the addition of dye, was necessary to achieve a strong correlation to the SNR batch test (see section Prediction of the SNR outcome using the CBB Panel Fluorescence Data and PLS modeling for modeling result). Only the initial fluorescence signal was needed since the fluorescence signal was stable over the 15 min reading period (Figure S6); bacteria can adapt to stressful environment within minutes.[52] On the basis of modeling performance, it was found that there was no advantage to using the fluorescence signals over a 15 min period (results not shown). This outcome was convenient, as it reduced the complexity and the amount of time needed to test a WW sample. The results in the panel on the left in Figure 1 show that after only 5 min of exposure to the WW sample and 1 min after the addition of the fluorescent dye, the change in fluorescence signal for the bacterial strains are remarkably different after exposure to the same WW sample. For example, the fluorescence signal of *Nitrosomonas europaea* and *Escherichia coli* increased by 86% and 27%, respectively, while the fluoresence signal of *Bacillus subtilis* and *Streptomyces laurentii* decreased by 14% and 19%, respectively, relative to the control sample. It is assumed that the observed differences in the fluorescence signals are due to many factors including the bacterial strain type, structure (Gram-negative vs Gram-positive), and the chemical composition of the WW sample (see section Prediction of the SNR outcome using the CBB Panel Fluorescence Data and PLS modeling for a more detailed discussion).

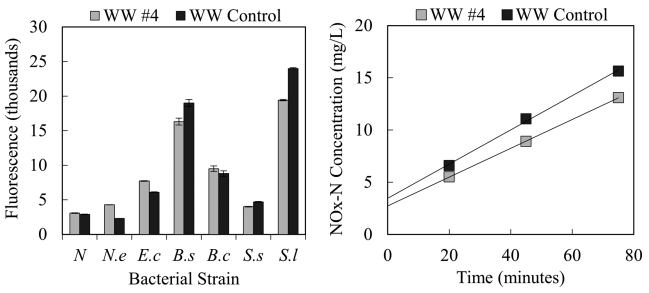

Figure 1. Left panel: Fluorescence data from the CBB panel for industrial WW sample #4 (gray bars) and Milli-Q water control (black bars). The fluorescence signals show the initial fluorescence (1 min after dye addition) for each of the seven bacterial strains: *Nitrospira* (*N*), *Nitrosomonas europaea* (*N.e*), *Escherichia coli* (*E.c*), *Bacillus subtilis* (*B.s*), *Bacillus cereus* (*B.c*), *Staphylococcus saprophyticus* (*S.s*), and *Streptomyces laurentii* (*S.l*). Right panel: SNR batch test results for industrial WW sample #4 (gray square symbols) and Milli-Q water control (black square symbols). The best-fit value of the slope corresponding to the NO_x-N (nitrate-N and nitrite-N) production rate was 0.1379 for WW sample #4 and 0.1638 for the control. The % SNR difference calculated for WW #4 was +6.35 and thus for this study is considered a "fail" sample.

Table 1. R^2 and Q^2 Values for Different Numbers of Principal Components (1 to 5) in the CBB to SNR PLS Model for 26 Industrial WW Samples[a]

Number of principal components used	R^2	Q^2
1	0.69	0.12
2	0.80	0.65
3	0.84	0.75
4	0.86	0.78
5	0.86	0.79

[a]WW samples #3 and #17 were excluded from the model due to the large squared residuals (outliers).

The change in concentration of NO_x-N (nitrate-N and nitrite-N) during the SNR batch test is shown in the panel on the right. The % SNR difference was calculated from the NO_x-N production rate (slope), VSS measurement (4370 mg/L), and average temperature via Equations 1 and 2. A linear regression analysis was used to capture the NO_x-N production rate since the expected change in the autotrophic bacterial population is negligible over the amount of time (75 min) required to run the test.[10] The % SNR difference for this WW sample was calculated to be +6.35, relative to the control, and thus is designated as a "fail" sample. Exactly the same sequence of testing was done for all of the other 27 industrial WW samples; those results are shown in Table S1. Of the 28 WW samples collected, 11 were designated as "pass" samples and 17 were designated as "fail" samples. Note that due to the high cost of reagents, only one SNR batch test was made for the majority of the WW samples. We are quite confident in the test reliability as a duplicate analysis of WW sample #2 gave values of +2.66 and +5.20 and a duplicate analysis of WW sample #18 gave values of +22.30 and +29.71.

3.2. Prediction of the SNR Outcome Using the CBB Panel Fluorescence Data and PLS Modeling. In order to develop an appropriate model that can use the CBB panel fluorescence data to predict the % SNR difference of an industrial WW sample, all of the results shown in Table S1 were modeled using PLS. After modeling (setup shown in Figure S3), it was determined that WW samples #3 and #17 had relatively large squared residuals (165 and 554, respectively) compared to the average (21 ± 26) and therefore were excluded. The effect of using between one and five principal components in the PLS model is shown in Table 1. When three principal components were used, which means the first three principal components (1, 2, and 3) are used in the model, the R^2 value was 0.84. According to Chin,[53] an R^2 value of 0.67 or greater substantially explains model variance. In order to capture the predictive ability of the model, the Q^2 value is reported.[54] When three principal components were used, the Q^2 value was 0.75. The Q^2 value is different than the R^2 value because the model uses a subset of the data ($6/7^{ths}$) as the training set to predict the remaining subset (1/7th) of the data; Q^2 is calculated the same way as R^2 but with both subsets combined.[53] In this way, Q^2 is an indicator of how well the model can predict the % SNR difference of new WW samples from just the CBB panel fluorescence data. In order to prevent overfitting, three principal components were

DOI: 10.1021/acs.est.9b04453
Environ. Sci. Technol. 2020, 54, 184−194

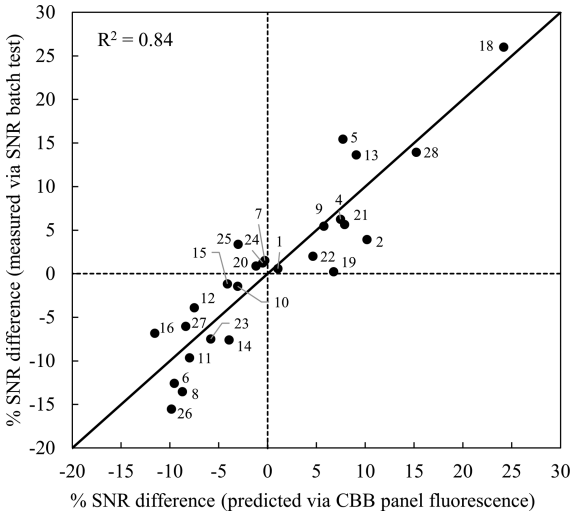

Figure 2. Comparison of the predicted % SNR difference values (from CBB panel fluorescence data) and the measured % SNR difference values (from SNR batch test) using PLS modeling and three principal components for 26 industrial WW samples. The solid diagonal line is included to indicate the perfect agreement between the two values. The Q^2 value (0.75) is close to the R^2 value (0.84) and therefore a testing set is not depicted (i.e., the testing data would look similar to the training data).

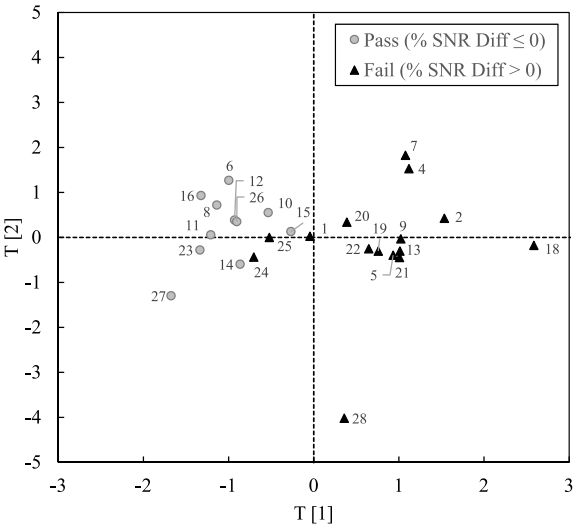

Figure 3. First and second principal component T-score plot for the X space of the CBB to SNR PLS model for 26 industrial WW samples. The greyed circle symbols represent the 11 WW samples with a "pass" rating (#6, #8, #10, #11, #12, #14, #15, #16, #23, #26, #27). The filled triangle symbols represent the 15 WW samples with a "fail" rating (#1, #2, #4, #5, #7, #9, #13, #18, #19, #20, #21, #22, #24, #25, #28).

used in this model as there was only a small increase in both the R^2 value (+0.02) and the Q^2 value (+0.03) when the fourth principal component was used. In the context of our application, achieving a Q^2 value of 0.75 is acceptable as there is significant value in determining whether or not nitrification inhibition is occurring; simply, a "pass" or "fail" determination is the most important. According to the literature, a Q^2 value greater than zero indicates that a model has "predictive relevance".[55] However, the degree of predictive relevance seems to be subjective and application dependent. For example, according to the *User Guide to SIMCA*[56] and Heneseler et al.,[57] a "large" degree of predictive relevance is characterized by a Q^2 value of greater than 0.5 and 0.35, respectively. In biological applications of PLS modeling involving metabolite analyses for diagnostic applications, Q2 values of 0.48 and 0.22 are deemed acceptable.[58,59] Those studies are relevant to this work since we are also investigating the impacts of metabolites/analytes (chemical compounds in WW samples) on bacteria that can be measured using fluorescence.

The effectiveness of using the CBB panel fluorescence data and PLS modeling to predict the % SNR difference is shown in Figure 2. The WW samples are closely aligned to the solid diagonal line (i.e., perfect agreement between the measured and predicted values). This means that the fluorescence signals from the CBB panel that were obtained in approximately 10 min can be used to predict the outcome of the SNR batch test, which takes approximately 4 h to complete. So as to pragmatically and easily allow for a 10 min test time of the CBB panel without the need for constantly culturing the strains, it is anticipated that future developments of this technology will involve preservation (e.g., using sugar films) of the strains which has been well documented in the literature.[60,61] As previously mentioned, it is of utmost importance to determine whether a sample is a "pass" or "fail", and therefore, the precise prediction of the % SNR difference may not be necessary. However, as the measured % SNR difference approaches the "pass-fail" criteria (which for this study was chosen to be zero), it becomes increasingly more difficult to predict. For example, WW samples #7, #20, #24, #25 are the only WW samples (of 26 samples) that were incorrectly predicted as "pass" samples; the measured % SNR difference values for these samples are +1.51, + 1.24, + 0.90, and +3.38, respectively, and the predicted % SNR difference values for these samples are −0.28, −0.51, −1.18, and −3.02, respectively. To better predict the values, specifically those that are close to the "pass-fail" criteria, more WW samples (preferably of varying compositions) should be collected and the results added to the model to further improve its predictive ability.

In order to gain insight into how the CBB panel fluorescence data predicts the % SNR difference, a T-score plot was generated and analyzed. The scores of the first and second principal component, the principal components which best explain variance in the training data, for each WW sample are displayed in Figure 3. By reducing the dimensionality to two (first and second score) using PLS modeling, the differences between "pass" and "fail" WW samples is evident. Figure 3 shows that the "pass" WW samples tend to cluster together on the left side of the plot, while the "fail" WW samples tend to be distributed in various mid-to-right and lower-right regions of plot. This distribution can be attributed to the broad differences in effects of varying chemical compounds on each bacterial strain. By analyzing each cluster ("pass", "fail") with a contribution plot, we can understand the behavior based on the fluorescence signal of each bacterial strain when exposed to a "pass" or "fail" WW sample.

The contribution plot for the PLS model is shown in Figure 4. The reader is referred to the *User Guide to SIMCA*[56] to understand how the contributions values are calculated. Generally, for WW samples with a "fail" rating, *Nitrospira*, *Escherichia coli*, and *Bacillus cereus* have fluorescence signals higher than the average (for each strain), while *Bacillus subtilis* has fluorescence signals lower than the average. Interestingly, there was no significant effect found for *Nitrosomonas europaea*, *Staphylococcus saprophyticus* and *Streptomyces laurentii*; the contribution values for these three strains were -3.58×10^{-3},

DOI: 10.1021/acs.est.9b04453
Environ. Sci. Technol. 2020, 54, 184−194

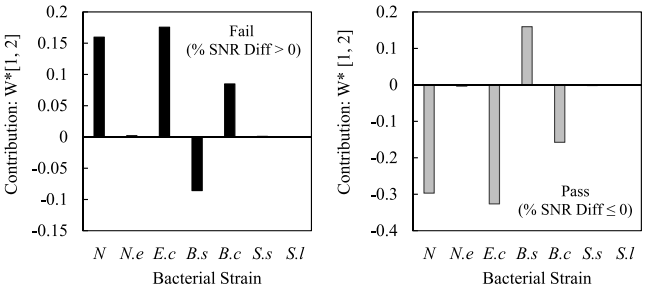

Figure 4. Contribution plot for the CBB to SNR PLS model. Average "fail" result (left) and "pass" result (right) of the seven bacterial strains (*Nitrospira* (*N*), *Nitrosomonas europaea* (*N.e*), *Escherichia coli* (*E.c*), *Bacillus subtilis* (*B.s*), *Bacillus cereus* (*B.c*), *Staphylococcus saprophyticus* (*S.s*), and *Streptomyces laurentii* (*S.l*)) measured as contributions for the first and second component. The weights without residuals (W*) are used. Contribution values greater than zero indicate a fluorescence signal that is greater than the average fluorescence signal for all WW samples, for that particular bacterial strain. Contribution values less than zero indicate the opposite (less than the average).

-1.77×10^{-3}, and $+0.12 \times 10^{-3}$ for "pass" and $+1.92 \times 10^{-3}$, $+0.95 \times 10^{-3}$, and -0.06×10^{-3} for "fail" samples, respectively.

This is a surpising result, particularly for *Nitrosomonas europaea*, since it is a prominent nitrifying bacterium; we hypothesize that due to its high settleability rate (these bacteria form strong bacterial clumps or large flocs), the fluorescence signals are not as reliable as the other strains. The results in Figure S1 confirm this hypothesis since the fluorescence signals for *Nitrosomonas europaea* display a downward trend as the WW sample number increases from left to right. We believe that this trend represents the settling of the bacteria as the microplate was analyzed (from WW sample #1 to #28). For WW samples with a "pass" rating, *Nitrospira*, *Escherichia coli*, and *Bacillus cereus* have fluorescence signals lower than the average (for each strain), while *Bacillus subtilis* has fluorescence signals higher than the average (the opposite of the "fail" rating). Again, no effect is seen with *Nitrosomonas europaea*, *Staphylococcus saprophyticus* and *Streptomyces laurentii*. Although we do not fully understand the reason as to why certain strains behave the way they do, previous research indicates that an increase in the fluorescence signal for *E. coli* is correlated with an increase in the amount of intracellular RNA.[62] It is our hypothesis that an increase in the intracellular RNA and hence an increase in the fluorescence signal is due to an increase in cellular activity which is triggered by specific chemical compounds in the WW samples. A decrease in the

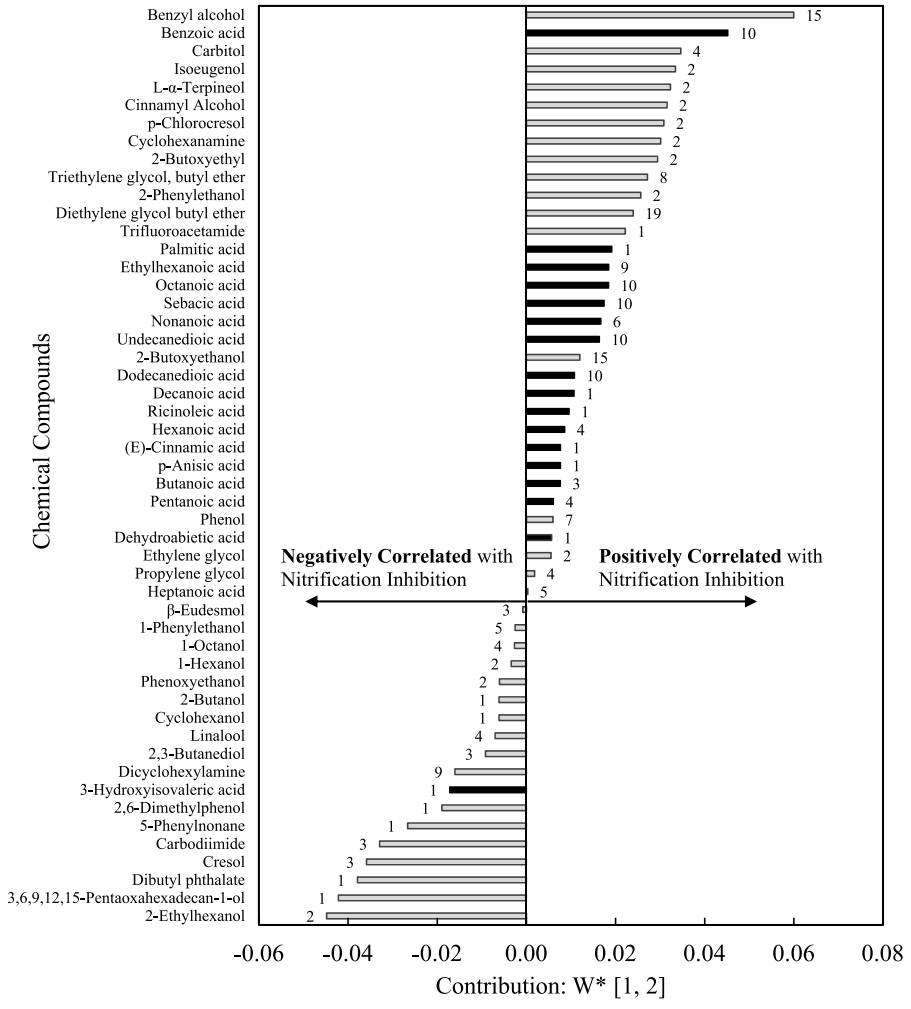

Figure 5. Contribution plot for the GC-MS to SNR PLS Model. The effect of 51 different chemical compounds from 19 WW samples on the % SNR difference are shown. The contributions of these 51 chemical compounds are shown for the first and second principal component; the weights without residuals (W*) are used. Dark bars (filled) are carboxylic acids, while light bars (greyed) are all other chemical compounds. The number beside each bar is the number of times that compound was detected in the 19 WW samples.

DOI: 10.1021/acs.est.9b04453
Environ. Sci. Technol. 2020, 54, 184−194

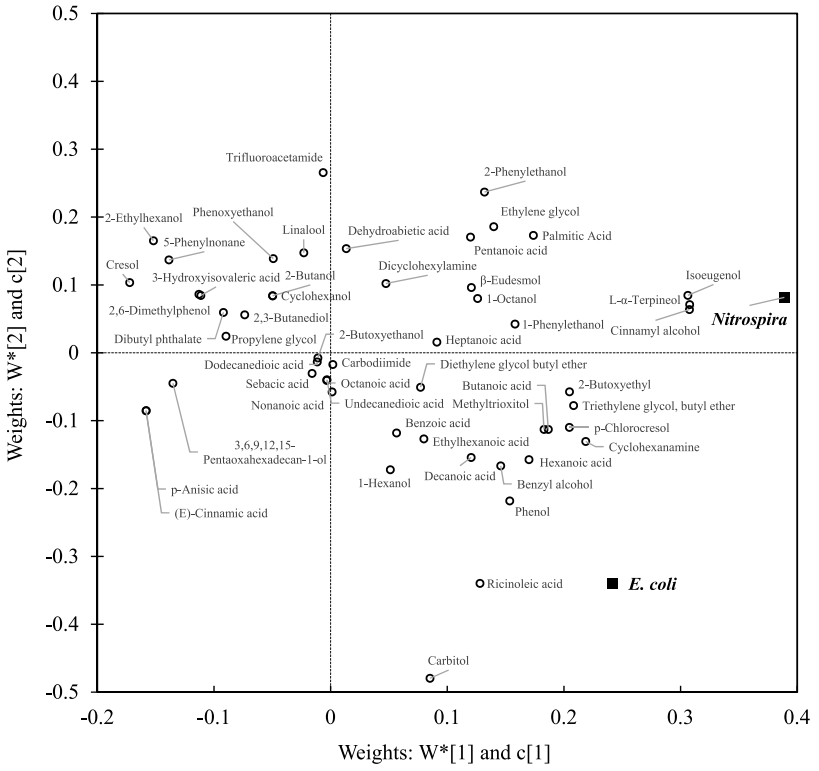

Figure 6. A weight biplot for the GC-MS to CBB PLS model. Positively correlated weights for the *X* space (GC-MS) and *Y* space (CBB) appear on the same side (left or right, top or bottom) of the plot. Negatively correlated weights appear on opposite sides. Weights that appear in the same quadrant are more strongly correlated. Similar to Figure 4 and Figure 5, the weights without residuals (W*) are used.

fluorescence signal is likely due to an increase in cellular membrane porosity.[26,29] Since the "live" fluorescent dye (SYTO 9) used in this commerically provided kit works by primarily binding to nucleic acids such as DNA and RNA (as previously mentioned),[29] when the cellular membrane porosity increases, the SYTO 9 dye is replaced with propidium iodide (present in the dye), effectively decreasing the fluorescence signal. However, we believe that these outcomes (increase in intracellular RNA, increase in membrane porosity) are not mutually exclusive and can occur simultaneously due to the many differences in the bacteria strains and their complex interactions with the wide range of chemical compounds present in each WW sample (see section 3.3 and 3.4 for details).

On the basis of the contribution results in Figure 4, it is interesting to note that of the four bacterial strains that contribute heavily to predicting the nitrification inhibition potential, two are Gram-negative (*Nitrospira*, *E. coli*) and two are Gram-positive (*Bacillus subtilis*, *Bacillus cereus*). Since both Gram-negative strains respond similarly with respect to each other when exposed to "pass" and "fail" samples, this may be one of many factors that can explain the differences in the fluorescence signals between strains. *Bacillus cereus* does not display the same effect as its Gram-positive counterpart, *Bacillus subtilis*, and therefore, the fluorescence signals are likely influenced by other factors (e.g., metabolism of specific chemical compounds) that may be bacterial strain specific. For example, it has been shown that approximately 30 genes for *Bacillus cereus* and 100 genes for *Bacillus subtilis* are transcribed upon exposure to environmental stress (e.g., acid stress) and therefore would react differently.[31] Gram-negative bacteria have a cell wall made of a thin peptidoglycan layer in comparison to Gram-positive bacteria,[63] and it has been reported that peptidoglycan may play a role in the permeability of the cell wall in bacteria that would affect which chemical compounds could enter the cell.[64] In some cases, certain chemical compounds such as surfactants (e.g., cetyltrimethylammonium bromide) have been shown to increase the permeability of bacterial cells.[12] Once permeabilized, intracellular enzymes can perform their functions more quickly by allowing free diffusion of small molecules through the membrane.[12] Another reason for the differences in the fluorescence signals between the strains could be due to the selective passage of chemical compounds through the hydrophilic Porins (channels) on the outer envelope of Gram-negative bacteria.[63] Gram-negative and Gram-positive bacteria are also known for their differences in regulating transcription and translation in response to the binding of riboswitches, which are stimulated in response to the binding of specific molecules.[65] Riboswitches generally attenuate transcription in Gram-positive bacteria and attenutate translation in Gram-negative bacteria.[66] Finally, researchers have shown that when bacterial cells are exposed to stressful environments that contain various metabolic toxins, the genes of the stress proteins are generally mutated which affects DNA and RNA synthesis.[30] Due to the many possible explanations for the differences in the fluorescence signals from strain to strain, future work will be done to better help understand the observed outcomes in this part of our study.

3.3. The Effect of Chemical Compounds on Nitrification Inhibition. The GC-MS to SNR PLS model was used to predict which chemical compounds are positively and negatively correlated with nitrification inhibition. This was made possible by using the setup shown in Figure S4 and analyzing the contribution plot. Nineteen WW samples were used in the model. Five of the WW samples (#17, #18, #21, #25, and #26)

DOI: 10.1021/acs.est.9b04453
Environ. Sci. Technol. 2020, 54, 184−194

were not used because they had GC-MS peak areas that were approximately 3 orders of magnitude lower than the average peak areas of all of the other WW samples (results not shown) and thus we were concerned that the results were unreliable. An additional four WW samples (#5, #15, #19, and #23) were not included (see Table S2) in the model as they fell outside of the 95% confidence interval for the squared prediction error and Hotelling's T^2 values. Two principal components were used in this PLS model with large cumulative R^2 and Q^2 values (0.83 and 0.41, respectively) indicating the possibility of using GC-MS to predict the nitrification inhibition potential of a WW sample.

The impact of each chemical compound on the nitrification inhibition potential is shown as a contribution plot in Figure 5. The chemical compounds with positive *x*-axis values (e.g., benzyl alcohol, benzoic acid) are positively correlated with nitrification inhibition, and the chemical compounds with negative *x*-axis values (e.g., 2,3-butanediol, linalool) are negatively correlated with nitrification inhibition. The numerical value beside each bar is the number of times that particular compound was detected by GC-MS. It is interesting to note that diethylene glycol butyl ether appears in every one of the 19 WW samples and benzyl alcohol and 2-butoxyethanol each appear in 15 of the samples. Also, of the 51 chemical compounds present in these 19 WW samples, eight chemical compounds appear in at least half (i.e., 10 out of 19) of the samples. Seventeen of the 33 chemical compounds that are positively correlated with nitrification inhibition are carboxylic acids (black filled bars). We hypothesize that this result is likely due to the high electronegativity and therefore polarity of carboxylic acids[67] and since WW bacteria tend to be more hydrophilic than hydrophobic.[68] For example, it is shown that octanoic acid and 1-octanol are positively and negatively correlated with nitrification inhibiton, respectively. Also, the observed effects of aromatic chemical compounds (benzoic acid, phenol, and *p*-chlorocresol) on nitrification inhibition are consistent with previous studies.[69−71] However, it is also shown that some aromatic chemical compounds such as cyclohexanol and cresol are negatively correlated with nitrification inhibition; we suspect that the competition between the chemical compounds plays a large role in the selective uptake in bacterial cells.

3.4. The Effect of Chemical Compounds on Bacteria Fluorescence Signal. The same 19 WW samples were used in a GC-MS to CBB PLS model (setup shown in Figure S5). In this model, we found that *E. coli* and *Nitrospira* were the only strains to have predictive relevance ($Q^2 > 0$) for all of the principal components analyzed (Table S3) and therefore, only the fluorescence signals from *Nitrospira* and *E. coli* were included. This result may be due to their Gram-negative membrane structure; it is hypothesized that these strains can better discriminate between the compounds present in a WW sample due to the selective passage of hydrophilic compounds through Porins into the cell.[63] Two principal components were used in this PLS model; the cumulative R^2 and Q^2 values were 0.73 and 0.14, respectively (see Table S4 for details on the other principal components). The large R^2 value with only two principal components indicates that this model can potentially be used to predict which chemical compounds are present in a WW sample based on the fluorescence signal of the two strains using a weight biplot (Figure 6). The low Q^2 value indicates that more WW samples need to be tested due to the large number of chemical compounds.

By analyzing the locations of the weights (left or right, top or bottom, diagonal) shown as empty circles for the chemical compounds and black squares for the strains, predictions can be made. For example, benzyl alcohol and pentanoic acid are present on the same side (right) of the weight biplot as *Nitrospira* and thus are positively correlated in the first principal component. However, benzyl alcohol is also present on the opposite side (bottom) of *Nitrospira* in the second principal component. This means that the presence of pentanoic acid is more likely to have a larger effect than benzyl alcohol on increasing the fluorescence signal of *Nitrospira*. In another example, *p*-anisic acid and 2-ethylhexanol are present on the opposite side (left) of the weight biplot as *E. coli* and thus are negatively correlated in the first principal component. In addition, 2-ethylhexanol is also present diagonally of *E. coli* indicating they are also negatively correlated in the second principal component. This means that 2-ethylhexanol is more likely to have a larger effect than *p*-anisic acid on decreasing the fluorescence signal of *E. coli*. Therefore, by measuring the fluorescence signals of *Nitrospira* and *E. coli* and after consulting the weight biplot, there is a strong potential to estimate which chemical compounds are present in a WW sample.

■ ASSOCIATED CONTENT

Supporting Information

The Supporting Information is available free of charge at https://pubs.acs.org/doi/10.1021/acs.est.9b04453.

Tables: CBB panel fluorescence data, GC-MS normalized integral peak area values, GC-MS to bacterial strain fluorescence, GC-MS to CBB (only *Nitrospira, E. coli*) PLS model information. Figures: Fluorescence comparison of each strain to the WW samples, SNR experimental setup, PLS model setups, fluorescence stability.(PDF)

■ AUTHOR INFORMATION

Corresponding Author

*Phone: 1-905-525-9140 extension 24011. E-mail: latulippe@mcmaster.ca.

ORCID

Carlos D. M. Filipe: 0000-0002-7410-3323

David R. Latulippe: 0000-0003-2873-0606

Notes

The authors declare no competing financial interest.

■ ACKNOWLEDGMENTS

This work was principally supported by the Voucher for Innovation and Productivity II program (Award 25160) from Ontario Centres of Excellence in combination with funding from Aevitas Inc (Brantford, Ontario). Additional funding was provided by the Natural Sciences and Engineering Research Council of Canada in the form of a Postgraduate Scholarship (to Patrick Morkus). From the Mobix Lab at McMaster University, we thank Ms. Laura Rossi for her help with Sanger sequencing of the bacterial strains. From the McMaster Regional Centre for Mass Spectrometry, we thank Dr. Kirk Green and Dr. Fan Fei for their guidance on running the GC-MS system and analyzing the results. From the City of Hamilton, we thank the operators at the Dundas Valley Wastewater Treatment Plant for providing the samples of return activated sludge that were used for the SNR batch tests.

DOI: 10.1021/acs.est.9b04453
Environ. Sci. Technol. 2020, 54, 184−194

REFERENCES

(1) Comeau, Y. (2008). Microbial metabolism. *Biological wastewater treatment: principles, modeling and design*. IWA/Cambridge University Press: London, *cap*, *2*, 9−32.

(2) Juretschko, S.; Timmermann, G.; Schmid, M.; Schleifer, K. H.; Pommerening-Röser, A.; Koops, H. P.; Wagner, M. Combined molecular and conventional analyses of nitrifying bacterium diversity in activated sludge: Nitrosococcus mobilis and Nitrospira-like bacteria as dominant populations. *Applied and environmental microbiology* **1998**, *64* (8), 3042−3051.

(3) Chain, P.; Lamerdin, J.; Larimer, F.; Regala, W.; Lao, V.; Land, M.; Hauser, L.; Hooper, A.; Klotz, M.; Norton, J.; Sayavedra-Soto, L.; Arciero, D.; Hommes, N.; Whittaker, M.; Arp, D. Complete genome sequence of the ammonia-oxidizing bacterium and obligate chemolithoautotroph Nitrosomonas europaea. *Journal of bacteriology* **2003**, *185* (9), 2759−2773.

(4) Henriques, I. D.; Love, N. G. Chemical inhibition of nitrification in activated sludge. *Biotechnology and bioengineering* **2004**, *85* (6), 683−694.

(5) Iwasaki, T., Takeno, T., Yamamoto, Y. (1988). *U.S. Patent No.* US4,770,694. U.S. Patent and Trademark Office, Washington, DC.

(6) Affatato, S.; Bersaglia, G.; Emiliani, D.; Foltran, I.; Toni, A. Sodium-azide versus ProClin 300: influence on the morphology of UHMWPE particles generated in laboratory tests. *Biomaterials* **2004**, *25* (5), 835−842.

(7) Sherine, B. Biocidal Efficiency of Organic Inhibitor in Cooling Water Systems. *International Journal of Research and Development in Pharmacy and Life Sciences* **2015**, *4* (2), 1400−1406.

(8) Urwin, C.; Richardson, J. C.; Palmer, A. K. An evaluation of the mutagenicity of the cutting oil preservative Grotan BK. *Mutat. Res., Genet. Toxicol. Test.* **1976**, *40* (1), 43−46.

(9) Ranade, V. V., Bhandari, V. M. (2014). *Industrial wastewater treatment, recycling and reuse*. Butterworth-Heinemann:

(10) Bye, C. M.; Jones, R. M.; Dold, P. L. Pragmatic nitrification inhibition testing for robust plant design. *Proceedings of the Water Environment Federation* **2012**, *2012* (12), 4222−4238.

(11) Farré, M.; Barceló, D. Toxicity testing of wastewater and sewage sludge by biosensors, bioassays and chemical analysis. *TrAC, Trends Anal. Chem.* **2003**, *22* (5), 299−310.

(12) D'Souza, S. F. Microbial biosensors. *Biosens. Bioelectron.* **2001**, *16* (6), 337−353.

(13) Pancrazio, J. J.; Whelan, J. P.; Borkholder, D. A.; Ma, W.; Stenger, D. A. Development and application of cell-based biosensors. *Ann. Biomed. Eng.* **1999**, *27* (6), 697−711.

(14) Kuhn, I., Colque-Navarro, P., Gabrielson, J., Iversen, A., McKenzie, J. D., Hart, M. C. (2013). *U.S. Patent No.* US8,551,921. U.S. Patent and Trademark Office, Washington, DC.

(15) Jung, Y.; Park, C. B.; Kim, Y.; Kim, S.; Pflugmacher, S.; Baik, S. Application of multi-species microbial bioassay to assess the effects of engineered nanoparticles in the aquatic environment: potential of a luminous microbial array for toxicity risk assessment (LumiMARA) on testing for surface-coated silver nanoparticles. *Int. J. Environ. Res. Public Health* **2015**, *12* (7), 8172−8186.

(16) Hsieh, C. Y.; Tsai, M. H.; Ryan, D. K.; Pancorbo, O. C. Toxicity of the 13 priority pollutant metals to Vibrio fisheri in the Microtox® chronic toxicity test. *Sci. Total Environ.* **2004**, *320* (1), 37−50.

(17) Rigol, A.; Latorre, A.; Lacorte, S.; Barceló, D. Bioluminescence inhibition assays for toxicity screening of wood extractives and biocides in paper mill process waters. *Environ. Toxicol. Chem.* **2004**, *23* (2), 339−347.

(18) Mamais, D.; Noutsopoulos, C.; Stasinakis, A. S.; Kouris, N.; Andreadakis, A. D. Comparison of bioluminescence and nitrification inhibition methods for assessing toxicity to municipal activated sludge. *Water Environ. Res.* **2008**, *80* (6), 484−489.

(19) Jönsson, K.; Grunditz, C.; Dalhammar, G.; Jansen, J. L. C. Occurrence of nitrification inhibition in Swedish municipal wastewaters. *Water Res.* **2000**, *34* (9), 2455−2462.

(20) Grunditz, C.; Gumaelius, L.; Dalhammar, G. Comparison of inhibition assays using nitrogen removing bacteria: application to industrial wastewater. *Water Res.* **1998**, *32* (10), 2995−3000.

(21) Grunditz, C.; Dalhammar, G. Development of nitrification inhibition assays using pure cultures of Nitrosomonas and Nitrobacter. *Water Res.* **2001**, *35* (2), 433−440.

(22) Kadlec, P.; Grbić, R.; Gabrys, B. Review of adaptation mechanisms for data-driven soft sensors. *Comput. Chem. Eng.* **2011**, *35* (1), 1−24.

(23) Kadlec, P.; Gabrys, B.; Strandt, S. Data-driven soft sensors in the process industry. *Comput. Chem. Eng.* **2009**, *33* (4), 795−814.

(24) Ohadi, S. K. (**2014**). *Development of Soft Sensors for Monitoring of Chinese Hamster Ovary Cell Processes*.

(25) Luccarini, L.; Porra, E.; Spagni, A.; Ratini, P.; Grilli, S.; Longhi, S.; Bortone, G. Soft sensors for control of nitrogen and phosphorus removal from wastewaters by neural networks. *Water Sci. Technol.* **2002**, *45* (4−5), 101−107.

(26) Oliver, J. D. The viable but nonculturable state in bacteria. *Journal of Microbiology* **2005**, *43* (1), 93−100.

(27) Kim, H. J.; Tango, C. N.; Chelliah, R.; Oh, D. H. Sanitization Efficacy of Slightly Acidic Electrolyzed Water against pure cultures of Escherichia coli, Salmonella enterica, Typhimurium, Staphylococcus aureus and Bacillus cereus spores, in Comparison with Different Water Hardness. *Sci. Rep.* **2019**, *9* (1), 4348.

(28) Diaz-Pascual, F.; Hartmann, R.; Lempp, M.; Vidakovic, L.; Song, B.; Jeckel, H.; Thormann, K. M.; Yildiz, F. H.; Dunkel, J.; Link, H.; Nadell, C. D.; Drescher, K. Breakdown of Vibrio cholerae biofilm architecture induced by antibiotics disrupts community barrier function. *Nature microbiology* **2019**, *4*, 1−10.

(29) Molecular Probes. (2003). *SYTO Green-Fluorescent Nucleic Acid Stains*.

(30) Welch, W. J. How cells respond to stress. *Sci. Am.* **1993**, *268* (5), 56−64.

(31) Desriac, N.; Broussolle, V.; Postollec, F.; Mathot, A. G.; Sohier, D.; Coroller, L.; Leguerinel, I. Bacillus cereus cell response upon exposure to acid environment: toward the identification of potential biomarkers. *Front. Microbiol.* **2013**, *4*, 284.

(32) Juretschko, S.; Timmermann, G.; Schmid, M.; Schleifer, K. H.; Pommerening-Röser, A.; Koops, H. P.; Wagner, M. Combined molecular and conventional analyses of nitrifying bacterium diversity in activated sludge: Nitrosococcus mobilis and Nitrospira-like bacteria as dominant populations. *Appl. Environ. Microbiol.* **1998**, *64* (8), 3042−3051.

(33) Antoniou, P.; Hamilton, J.; Koopman, B.; Jain, R.; Holloway, B.; Lyberatos, G.; Svoronos, S. A. Effect of temperature and pH on the effective maximum specific growth rate of nitrifying bacteria. *Water Res.* **1990**, *24* (1), 97−101.

(34) Arp, D. J.; Sayavedra-Soto, L. A.; Hommes, N. G. Molecular biology and biochemistry of ammonia oxidation by Nitrosomonas europaea. *Arch. Microbiol.* **2002**, *178* (4), 250−255.

(35) Reinthaler, F.F; Posch, J; Feierl, G; Wust, G; Haas, D; Ruckenbauer, G; Mascher, F; Marth, E Antibiotic resistance of E. coli in sewage and sludge. *Water Res.* **2003**, *37* (8), 1685−1690.

(36) Salehizadeh, H.; Yan, N. Recent advances in extracellular biopolymer flocculants. *Biotechnol. Adv.* **2014**, *32* (8), 1506−1522.

(37) Bartoszewicz, M.; Czyżewska, U. Spores and vegetative cells of phenotypically and genetically diverse Bacillus cereus sensu lato are common bacteria in fresh water of northeastern Poland. *Can. J. Microbiol.* **2017**, *63* (12), 939−950.

(38) Börjesson, S.; Matussek, A.; Melin, S.; Löfgren, S.; Lindgren, P. E. Methicillin-resistant Staphylococcus aureus (MRSA) in municipal wastewater: an uncharted threat? *J. Appl. Microbiol.* **2010**, *108* (4), 1244−1251.

(39) Ferreira, A. M.; Bonesso, M. F.; Mondelli, A. L.; de Souza, M. D. L. R. Identification of Staphylococcus saprophyticus isolated from patients with urinary tract infection using a simple set of biochemical tests correlating with 16S−23S interspace region molecular weight patterns. *J. Microbiol. Methods* **2012**, *91* (3), 406−411.

DOI: 10.1021/acs.est.9b04453
Environ. Sci. Technol. 2020, 54, 184−194

(40) Abou-Elela, S. I.; Kamel, M. M.; Fawzy, M. E. Biological treatment of saline wastewater using a salt-tolerant microorganism. *Desalination* **2010**, *250* (1), 1−5.
(41) Doi, K.; Fujino, Y.; Nagayoshi, Y.; Ohshima, T.; Ogata, S. Complete genome sequence of thiostrepton-producing *Streptomyces laurentii* ATCC 31255. *Genome announcements* **2016**, *4* (3), e00360−16.
(42) Hozzein, W. N.; Ahmed, M. B.; Tawab, M. S. A. Efficiency of some actinomycete isolates in biological treatment and removal of heavy metals from wastewater. *Afr. J. Biotechnol.* **2012**, *11* (5), 1163−1168.
(43) Smejkalova, M.; Mikanova, O.; Boruvka, L. Effects of heavy metal concentrations on biological activity of soil micro-organisms. *Plant, Soil Environ.* **2003**, *49* (7), 321−326.
(44) U.S Environmental Protection Agency Office of Water. (2001). *Total, Fixed, and Volatile Solids in Water, Solids, and Biosolids*. Washington, DC.
(45) Hoilijoki, T. H.; Kettunen, R. H.; Rintala, J. A. Nitrification of anaerobically pretreated municipal landfill leachate at low temperature. *Water Res.* **2000**, *34* (5), 1435−1446.
(46) Bourrain, M.; Achouak, W.; Urbain, V.; Heulin, T. DNA extraction from activated sludges. *Curr. Microbiol.* **1999**, *38* (6), 315−319.
(47) Seyhi, B.; Drogui, P.; Buelna, G.; Blais, J. F. Removal of bisphenol-A from spiked synthetic effluents using an immersed membrane activated sludge process. *Sep. Purif. Technol.* **2012**, *87*, 101−109.
(48) Raboni, M.; Torretta, V.; Viotti, P.; Urbini, G. Calculating specific denitrification rates in pre-denitrification by assessing the influence of dissolved oxygen, sludge loading and mixed-liquor recycle. *Environ. Technol.* **2014**, *35* (20), 2582−2588.
(49) Government of Canada. (2012, June 29). *Wastewater Systems Effluent Regulations*. Retrieved from Justice Laws: https://laws-lois.justice.gc.ca/eng/regulations/sor-2012-139/fulltext.html.
(50) Holly, D. (2010). *Online Process Monitoring of Part Manufacturing Using MVA*. McMaster University library: Hamilton.
(51) Höskuldsson, A. A combined theory for PCA and PLS. *J. Chemom.* **1995**, *9* (2), 91−123.
(52) Heipieper, H. J.; Fischer, J.; Meinhardt, F. Cis−trans isomerase of unsaturated fatty acids: an immediate bacterial adaptive mechanism to cope with emerging membrane perturbation caused by toxic hydrocarbons. *Cellular Ecophysiology of Microbe: Hydrocarbon and Lipid Interactions* **2018**, 385−395.
(53) Chin, W. W. The partial least squares approach to structural equation modeling. *Modern methods for business research* **1998**, *295* (2), 295−336.
(54) Umetrics. (n.d.). *F.A.Q SIMCA-P and Multivariate Frequently Asked Questions, version 1.01*.
(55) Hair, Jr, J. F., Hult, G. T. M., Ringle, C., Sarstedt, M. (2016). *A primer on partial least squares structural equation modeling (PLS-SEM)*. Sage Publications:
(56) MKS Umetrics. (2012). *User Guide to SIMCA, Version 13*.
(57) Henseler, J., Ringle, C. M., Sinkovics, R. R. (2009). The use of partial least squares path modeling in international marketing. In *New challenges to international marketing* (pp 277−319). Emerald Group Publishing Limited:
(58) Slupsky, C. M.; Steed, H.; Wells, T. H.; Dabbs, K.; Schepansky, A.; Capstick, V.; Faught, W.; Sawyer, M. B. Urine metabolite analysis offers potential early diagnosis of ovarian and breast cancers. *Clin. Cancer Res.* **2010**, *16* (23), 5835−5841.
(59) Ubhi, B. K.; Riley, J. H.; Shaw, P. A.; Lomas, D. A.; Tal-Singer, R.; MacNee, W.; Griffin, J. L.; Connor, S. C. Metabolic profiling detects biomarkers of protein degradation in COPD patients. *Eur. Respir. J.* **2012**, *40* (2), 345−355.
(60) Krumnow, A. A.; Sorokulova, I. B.; Olsen, E.; Globa, L.; Barbaree, J. M.; Vodyanoy, V. J. Preservation of bacteria in natural polymers. *J. Microbiol. Methods* **2009**, *78* (2), 189−194.
(61) Jahanshahi-Anbuhi, S.; Pennings, K.; Leung, V.; Liu, M.; Carrasquilla, C.; Kannan, B.; Li, Y.; Pelton, R.; Brennan, J. D.; Filipe, C. D. M. Pullulan encapsulation of labile biomolecules to give stable bioassay tablets. *Angew. Chem., Int. Ed.* **2014**, *53* (24), 6155−6158.
(62) Morkus, P.; Zolfaghari, M.; Parrello, D.; Csordas, M.; Malikov, M.; Rose, J.; Choi, K. B.; Filipe, C. D.M.; Latulippe, D. R. Optimization of microorganism preservation conditions for the development of an acute toxicity bioassay for biocides. *Chemosphere* **2019**, *221*, 45−54.
(63) Denyer, S. P.; Maillard, J. Y. Cellular impermeability and uptake of biocides and antibiotics in Gram-negative bacteria. *J. Appl. Microbiol.* **2002**, *92*, 35S−45S.
(64) Burman, L. G.; Nordström, K.; Bloom, G. D. Murein and the outer penetration barrier of Escherichia coli K-12, Proteus mirabilis, and Pseudomonas aeruginosa. *Journal of bacteriology* **1972**, *112* (3), 1364−1374.
(65) Waters, L. S.; Storz, G. Regulatory RNAs in bacteria. *Cell* **2009**, *136* (4), 615−628.
(66) Fernandez, J.; Yaman, I.; Huang, C.; Liu, H.; Lopez, A. B.; Komar, A. A.; Caprara, M. G.; Merrick, W. C.; Snider, M. D.; Kaufman, R. J.; Lamers, W. H.; Hatzoglou, M. Ribosome stalling regulates IRES-mediated translation in eukaryotes, a parallel to prokaryotic attenuation. *Mol. Cell* **2005**, *17* (3), 405−416.
(67) Siggel, M. R.; Streitwieser, A.; Thomas, T. D. The role of resonance and inductive effects in the acidity of carboxylic acids. *J. Am. Chem. Soc.* **1988**, *110* (24), 8022−8028.
(68) Zita, A.; Hermansson, M. Determination of bacterial cell surface hydrophobicity of single cells in cultures and in wastewater in situ. *FEMS Microbiol. Lett.* **1997**, *152* (2), 299−306.
(69) Kim, Y. M.; Park, D.; Lee, D. S.; Park, J. M. Inhibitory effects of toxic compounds on nitrification process for cokes wastewater treatment. *J. Hazard. Mater.* **2008**, *152* (3), 915−921.
(70) McCarty, G. W.; Bremner, J. M. Effects of Phenolic Compounds on Nitrification in Soil 1. *Soil Science Society of America Journal* **1986**, *50* (4), 920−923.
(71) Gutierrez, M.; Etxebarria, J.; De Las Fuentes, L. Evaluation of wastewater toxicity: comparative study between Microtox® and activated sludge oxygen uptake inhibition. *Water Res.* **2002**, *36* (4), 919−924.

DOI: 10.1021/acs.est.9b04453
Environ. Sci. Technol. 2020, 54, 184−194